D11

N79-27081

ANALYTICAL AND SCALE MODEL RESEARCH AIMED AT IMPROVED HANG GLIDER DESIGN

Ilan Kroo and Li-Shing Chang
Stanford University

SUMMARY

A program of research on the aerodynamics, aeroelasticity, and stability of hang gliders has recently begun at Stanford University with support from NASA. The research consists of a theoretical analysis which attempts to predict aerodynamic characteristics using lifting surface theory and finite-element structural analysis as well as an experimental investigation using 1/5-scale elastically similar models in the NASA Ames 2 m x 3 m (7' x 10') wind tunnel. Experimental data will be compared with theoretical results in the development of a computer program which may be used in the design and evaluation of ultra-light gliders.

This paper describes the goals and general procedures of the investigation begun in January 1979.

INTRODUCTION

In recent years the performance and variety of hang glider designs have increased dramatically. Flight conditions and demands that are placed on hang gliders are very different from those encountered by older designs. Whereas lift-to-drag ratios of 3 were common not long ago, some present designs achieve glide ratios of close to 10 and have been flown cross country for 160 km (100 mi) at altitudes as high as 6000 m (19,000 ft.) (Ref. 1). In addition to (often turbulent) thermal flying, increased controllability has made limited aerobatic maneuvers possible. Several years ago the results of NASA wind tunnel studies of the Rogallo wing (Ref. 2-7) in the 1960's could be used to obtain some idea of the characteristics of new designs. Although not all flight regimes and relevant parameters were thoroughly investigated, the data that did exist proved useful. The hang glider has evolved, however, to the point that these original investigations can no longer be applied. The flight characteristics of modern hang gliders (Ref. 8) with spans extending to 31 m (36 ft.), aspect ratios from 5 to 7.6 and sails with low billow and sweep, cannot be estimated from these data for the high billow (4 - 5 degrees), low aspect ratio (2.5) "standards". Information on the aerodynamic characteristics of present designs is almost entirely qualitative, deduced from limited flight tests of new designs.

Many problems that have been encountered might have been prevented had such data been available. Pitch-down divergence at low angles of attack continues to be an important problem. Thirty percent of fatalities in 1976 involved full-luffing dives from altitudes in excess of 60 m (200 ft.) (Ref. 9) although recovery is theoretically possible in less than 15 m (50 ft.) (Ref. 10). Statistics from hang gliding accidents in 1977 and 1978 show that, despite a more

thorough testing program pursued by the industry in the last few years, such instabilities are all too common even up to the present time.

Work was begun in January 1979 on a program of research aimed at providing quantitative tools for use in the design and evaluation of modern hang gliders. The investigation consists of two concurrent and closely integrated phases:

1) Basic force and moment measurements will be made on scale models in one of the 2 m x 3 m wind tunnels at NASA Ames Research Center. Models are being constructed that will reproduce the geometric, elastic, and aerodynamic properties of a representative class of modern glider.

2) A computer program, based on the best available analytic tools from potential aerodynamics and finite-element structural methods, for predicting the measured airloads with static aeroelastic corrections is being developed. After refinement by comparison with the tests, this program will be promulgated for the analysis of future glider designs.

As this research is to be conducted over the next two years, this paper describes the goals and general approach of the project with results to be published at a later date.

WIND TUNNEL TESTS

Models

Planned wind tunnel tests consist of measurements of the basic forces and moments on a group of 1/5-scale models at Reynold's numbers very close to the full scale value.

Although there exist today a wide variety of hang glider designs and it is no longer possible to test a "standard" configuration and use the results to predict universal characteristics for these aircraft, sufficient similarity does exist so that certain characteristics may be determined from tests on a limited number of models and applied to many other designs with similar features. In this way, good approximations to the properties of such gliders may be obtained from tests on a small group with different, but carefully selected, geometries. The models selected span a wide range of glider types, from the older Rogallo-type "standards" to more recent "intermediate" and high performance designs. (See Table 1). The effect on overall aerodynamic characteristics of various wing tip geometries, sail planforms, and camber and twist distributions common to many gliders will be determined from tests on this group of models.

The importance of elastic scaling has been demonstrated recently (Ref. 11). The flight characteristics of gliders are seen to vary considerably with changes in loading. This is caused by the flexibility of the frame and deformation of the sail of these ultralight gliders. For this reason, it is important that scale models be constructed in such a way as to remain geometrically similar to full size gliders under corresponding loads.

Another key assumption underlying the design of flexible models is the attainment of full-scale Reynolds' number, Re. This is because rather complex

separated-flow effects are anticipated at the larger values of α and β. Since available wind tunnels operate at essentially sea-level conditions, it follows that any resultant force, F_m, experienced by the model must equal the corresponding F_f at full scale. (Mach number effects are negligible at these "microsonic speeds.")

Force equality can be reasoned from the fact that:

$$Re_m = Re_f$$

where the product of speed and typical length, $V\ell$, must be the same at both scales. With air densities:

$$\rho_m = \rho_f$$

and forces proportional to $\rho V^2 \ell^2$, then:

$$F_m = F_f$$

The combination of equal force and equal strain requirements lead to difficulties in the construction of elastically scaled models. Consider that both the model and full scale gliders are constructed of tubes and cables of approximately circular cross sections of radius r, supporting the fabric sails. Since r should be proportional to ℓ for aerodynamic similarity, the strains in these tubes are proportional to $Fr\ell/EI$ or to Fr^2/EI, with EI the familiar bending rigidity. The severe requirement on model construction is to ensure

$$\left(\frac{r^2}{EI}\right)_m = \left(\frac{r^2}{EI}\right)_f$$

For a typical glider, assembled of thin-walled aluminum tubes, this quantity is of the order 10^{-7} N^{-1} (4×10^{-7} lb.$^{-1}$). If the same construction and material were employed on the model, one would get

$$\left(\frac{r^2}{EI}\right)_m = \left(\frac{\ell_f}{\ell_m}\right)^2 \left(\frac{r^2}{EI}\right)_f$$

This factor of 25 at one-fifth scale is quite unacceptable. Since weight is not believed to be a very significant factor, the situation can be alleviated by going to solid-section cylinders of stiffer material on the model. Models constructed of steel in this manner approach the desired stiffness:

$$\left(\frac{r^2}{EI}\right)_m = 3.4 \left(\frac{r^2}{EI}\right)_f$$

It appears that the requirement of equal strains, therefore, can only be met by some relaxation of the Reynolds number requirement. The following values correspond to the model construction above:

$$\frac{Re_m}{Re_f} = .53$$

This difference is not large and can be reduced further with the use of tubes and cables of slightly larger than scaled radii.

Especially for newer hang glider designs with low billow, it is important to duplicate the stretching of the fabric sail as well as the bending of frame elements. This requirement may be seen approximately as follows.

Requiring equal strains in the model and full-scale glider sails, $\varepsilon_m = \varepsilon_f$, for geometric similarity implies that

$$\varepsilon = \frac{\sigma}{E} = \frac{p(x)dx}{E\ dA} = \frac{p(x)dx}{Et\ dx} = \frac{F}{Et\ell}$$

is the same at both scales. Now since $\ell_m = \frac{1}{5}\ell_f$ and from above we have let $F_m = 1/3.4\ F_f$ we require that $(Et)_m = 1.8\ (Et)_f$. This can be achieved with the appropriate choice of Dacron fabric. Values of Et for Dacron sails are given in reference 24, from which it can be seen that the proper $(Et)_m$ may be achieved with two layers of material slightly lighter than that used on full-scale gliders.

Data Reduction

From measurements of the basic forces and moments on these models, the following performance coefficients and static stability derivatives can be calculated.

$$C_L \quad C_D \quad C_m \quad C_{m_\alpha} \quad C_{\ell_\beta} \quad C_{n_\beta}$$

Data will be obtained generally at angles of attack, α from -45^o through stall and at sideslip angles β to $\pm 20^o$. Tests will be conducted at various pressures to obtain data on the presumably significant variation of these quantities with the dynamic pressure, q (elastic effects). Test results will be corrected for jet blockage and wall effects.

Much of this data could be used immediately for design purposes with little intermediate manipulation. With the use of data on pitching moment coefficient, the longitudinal equations of motion may be numerically integrated to show the effectiveness of "weight-shift" control, including required bar pressures (stick forces), under various flight conditions. Stall, dive recovery, and other aspects of longitudinal motion will be analyzed. A similar analysis for lateral motion, taking account of the unusually large coupling between longitudinal and lateral modes associated with hang gliders, will also be carried out. At the present time, the first wind tunnel model is being constructed at the machine shop facilities at Stanford. The frame will have two possible nose

angles and by attaching different sails many configurations may be tested. Although a final list of configurations to be tested has not yet been determined, a tentative group of test models is described in table 1.

THEORETICAL ANALYSIS

In conjunction with the testing program, theoretical aerodynamic and aeroelastic methodology is being applied toward the development of a computer program which will undertake to predict some or all of the quantities measured in the experimental portion of the project.

Several theoretical treatments of "parawing" aerodynamics were published in the 1960's (e.g. Ref. 12-14). Lifting surface theory was used to predict lift and moment of various parawing configurations with the assumption of a particular mode shape (generally taken to be a portion of a right circular cone). Induced and profile drags and the effects of rigid leading edges were treated. Recent experimental work (Ref. 11) has shown, however, that changes in sail shape with angle of attack and dynamic pressure are extremely important, especially for current hang glider designs. Thus, not only is the assumption of conical canopy shape no longer valid, but no rigid analytic assumption of mode shape can be used.

The approach taken in the present analysis consists of two major parts:

1) The determination of airloads for a prescribed mode shape, and
2) The flexible structural response to this calculated loading, resulting in a new approximation for canopy shape.

The iterated procedure, shown schematically in Fig. 1, is used to obtain a solution for pressure distribution without the need for specifying the exact sail shape initially.

From these predicted airloads, force and moment coefficients may be calculated and compared with experimental results.

Aerodynamics

Linearized, steady, lifting-surface theory for incompressible flow is used in the prediction of aerodynamic loads on the glider. Under such conditions the flow over the glider satisfies Laplace's equation: $\nabla^2\phi = 0$ which may be solved with the use of vortex-lattice or kernel-function methods. The approach taken here utilizes the former method described by Woodward and Rubbert (Refs. 15,16) with a code by Nathman (Ref. 17) used at Stanford's computing facilities.

The sail is divided into finite elements as shown in Fig. 2. Each element is idealized as a flat panel of constant doublet strength, K, defined as the discontinuity in potential between the upper and lower surfaces,

$$K = \phi_\ell - \phi_u$$

As shown in the appendix, this leads to the following expression for the velocity induced at points outside this surface

$$\{V\} = \frac{1}{4\pi} [C]\{K\}$$

where $[C]$ is the aerodynamic influence matrix described in the appendix. The doublet strength for each panel is chosen so that the flow at the surface of the glider is tangent (zero sail porosity). This condition is satisfied if the normal velocity induced by the system of doublets just cancels the free-stream normal velocity:

$$[C_n]\{K\} = -4\pi \{n \cdot V_\infty\}$$

Since the surface normals and influence matrix may be computed from the assumed sail geometry and since the free-stream velocity is given, the value of K can be calculated over the surface.

Once K is known, the vorticity on the surface is given by:

$$\gamma = n \times \nabla K$$

and the loading:

$$\Delta p(x) = \rho V \times \gamma$$

These pressures are then used to calculate the desired force and moment coefficients according to standard definitions (cf. Ref. 18). The procedure is summarized in Fig. 3.

Figs. 4-6 show the preliminary results of this theory applied to some simple planforms for which experimental data is available. (Ref. 19,20). Agreement is close although effects of leading edges and deviation from conical geometry are not considered.

It should be noted that these results are the predictions of the aerodynamic portion of the program only. A rigid mode shape is assumed and so agreement with experiment can only be expected at intermediate α. The combination of this portion of the program and the structural analysis described below is presently underway and results are not yet available.

This analysis does not include the effect of pilot, cable or frame interference. It applies only to unseparated flow and does not include viscous effects. Corrections to the first stage of the analysis, taking these effects into account, are being studied and can, hopefully, be implemented in later work.

Structural Analysis

The sail and frame of a hang glider constitute a rather flexible structure assumed to be in a state of quasi-static equilibrium. Tension members, axially loaded beams, bending members, and membrane surfaces are all involved, with clearly defined modal connections. It is evident that the finite-element method of static, structural analysis is the only feasible way of representing and balancing the complete system of internal and external loads.

The approach taken here involves an analysis of the glider frame by classical methods and modelling of the sail as a membrane with very small flexural rigidity. The procedure is diagrammed in Fig. 7.

An incremental loading technique as described by Turner et al. (Ref. 21) is used to predict the response of the entire structure to the given applied load. The pressure distribution given by the aerodynamic portion of the analysis is broken down into small increments and the change in shape due to this incremental load is calculated. This is done by expressing the pressure, Δp_i, over each panel in terms of equivalent nodal loads, F_i, and calculating the displacement, D_i, of the nodes by the relation:

$$\{F\} = [S]\{D\}$$

Here, $[S]$ is a stiffness matrix, made up of a linear, elastic part $[S_e]$ which accounts for sail stretching (despite the anisotropic stretching behavior of textile materials, the glider sail is assumed isotropic for the early stage of the investigation) and a non-linear geometric part $[S_g]$ which depends on the geometry and initial tension. The addition of this geometric stiffness to the conventional stiffness matrix allows the non-linear strain-displacement relations associated with this large displacement problem to be incorporated in an approximate manner.

A method described by Argyris (Ref. 22) is adapted here to generate the geometric stiffness matrix. This method assumes a linear strain-displacement relationship within the elements and is considerably simpler than conventional techniques which require calculation of the strain energy (cf. Ref. 23).

At each step the geometric stiffness matrix is updated and nodal forces and incremental displacements calculated. After the step-by-step process is completed, the incremental displacements are summed to obtain a new mode shape which is then used as input to the aerodynamic program for another iteration.

A code based on this approach has been developed and is presently being checked by comparison with test cases for which analytic solutions are possible. Preliminary work indicates agreement to within a few percent in displacement although further work is needed to assure convergence in some cases.

Results from the experimental portion of the investigation will be used to establish the theoretical results' range of validity and will guide efforts to incorporate the effects of viscosity, interference, leading-edge suction, and other phenomena in the analytical portion of the research.

CONCLUDING REMARKS

The theory presented here is intended to provide a general idea of some of the methods to be used in this investigation. Much work is required before the analysis can properly take account of the complex aerodynamic and aeroelastic effects associated with modern hang gliders. At the time of this writing, the aerodynamic and structural routines have not been combined although it is expected that this will accomplished shortly. Wind-tunnel models are presently being fabricated for tests to be conducted later this year. Results from both the theoretical and experimental parts of this research will be published as they become available.

APPENDIX

Aerodynamic Influence Matrix Calculation

Expressing the velocity perturbation potential, $\phi(P)$, at a point P, in terms of the value of ϕ and its normal derivative $\frac{\partial \phi}{\partial n}$, on the fluid boundary by Green's theorem:

$$\phi(P) = \int_S \frac{\partial \phi(P')}{\partial n_s} \left(\frac{-1}{4\pi r}\right) ds + \int_S \phi(P') \frac{\partial}{\partial n_s} \left(\frac{1}{4\pi r}\right) ds$$

where r is the distance between P and P', a point on the boundary, S.

If the sail is taken to be a 2-dimensional surface, then $n_u = - n_\ell$ and, in order that the flow be tangent to the surface,

$$\frac{\partial \phi_u}{\partial n_u} = - \frac{\partial \phi_\ell}{n_\ell}$$

so;

$$\phi(P) = \int_S (\phi_u - \phi_\ell) \frac{\partial}{\partial n_u} \left(\frac{1}{4\pi r}\right) ds - \int_S K \frac{\partial}{\partial n_u} \left(\frac{1}{4\pi r}\right) ds$$

and

$$V(P) = \int_S VK \left(\frac{1}{4\pi}\right) \frac{\partial}{\partial n} \left(\frac{1}{r}\right) ds$$

If K is assumed constant over each of the panels S_j, then:

$$V(P) = \sum_j \frac{K_i}{4\pi} \left(- \int_s V \frac{\partial}{\partial n} \left(\frac{1}{r} \right) ds; \right)$$

The aerodynamic influence coefficient of the region S_j on the point P_i is thus defined as:

$$C_{ij} = - \int_{sj} \nabla \frac{\partial}{\partial n} \left(\frac{1}{r} \right) ds;$$

so:

$$V(P_i) \equiv V_i = \frac{1}{4\pi} K_j C_{ij}$$

Expressing this velocity at several points in matrix notation:

$$\{V\} = \frac{1}{4\pi} [C] \{K\}$$

REFERENCES

1. "Hang Gliding Magazine" (Formerly "Ground Skimmer"), Dec. 1973-Feb. 1979, a Monthly publication of the Unites States Hang Glider Association.

2. Johnson, Joseph L., Jr., "Low-Speed Wind-Tunnel Investigation to Determine the Flight Characteristics of a Model of a Parawing Utility Vehicle," NASA TN D-1255, 1962.

3. Johnson, Joseph L., Jr., and Hassell, James L., Jr., "Full-Scale Wind-Tunnel Investigation of a Flexible-Wing Manned Test Vehicle," NASA TN D-1946, 1963.

4. Naeseth, Roger L., and Gainer, Thomas G., "Low-Speed Investigation of the Effects of Wing Sweep on the Aerodynamic Characteristics of Parawings Having Equal-Length Leading Edges and Keel," NASA TN D-1957, 1963.

5. Bugg, Frank M., "Effects of Aspect Ratio and Canopy Shape on Low-Speed Aerodynamic Characteristics of 50° Swept Parawings," NASA TN D-2922, July 1965.

6. Croom, Delwin, R., Naeseth, Roger L., and Sleeman, William C., Jr., "Effects of Canopy Shape on Low-Speed Aerodynamic Characteristics of a 55° Swept Parawing with Large-Diameter Leading Edges," TN D-2551, Dec. 1964.

7. Johnson, Joseph L., Jr., "Low-Speed Force and Flight Investigations of a Model of a Modified Parawing Utility Vehicle," NASA TN D-2492, March 1965.

8. Hang Glider Design Catalog, Ground Skimmer, December 1975.

9. Wills, R.V., "Accident Summaries", Hang Gliding, 1974-1978.

10. Jones, R.T., "Dynamics of Ultralight Aircraft: Dive Recovery of Hang Gliders," May 1977, NASA TM X-73229.

11. Discussion with Robert Ormiston, NASA Ames Research Center, regarding results of full-scale tests in settling chamber of #2 7'x 10' wind tunnel at Ames, June 1977.

12. Mendenhall, M.R., Spangler, S.B., and Nielsen, J.N., "Investigation of Methods for Predicting the Aerodynamic Characteristics of Two-Lobed Parawings," NASA CR-1166, Sept. 1968.

13. Polhamus, Edward C., and Naeseth, Roger L., "Experimental and Theoretical Studies of the Effects of Camber and Twist on the Aerodynamic Characteristics of Parawings Having Nominal Aspect Ratios of 3 and 6," NASA TN D-972, 1963.

14. Nielsen, Jack N., and Burnell, Jack A., "Theoretical Aerodynamics of Flexible Wings at Low Speeds: Engineering Method for Estimating Parawing Performance, Final Report, Feb. - Nov. 1965," VIDYA-209, Dec. 1965.

15. Woodward, F.A., "Analysis and Design of Wing-Body Combinations at Subsonic and Supersonic Speeds," J. Aircraft, 5:528-34.

16. Rubbert, P.E., "Theoretical Characteristics of Arbitrary Wings by a Non-Planar Vortex Lattice Method," Boeing Co., Rep. D-6-9244, 1964.

17. Nathman, J.K., "Delta Wings in Incompressible Flow," AIAA 13th Annual Meeting, 1977.

18. Ashley, H., Engineering Analysis of Flight Vehicles, Addison-Wesley Publishing Co., Reading, Mass., 1974, (Sects. 3.1, 3.2, 8.2 etc).

19. Turnell, J.A., and Nielsen, J.N., "Aerodynamics of Flexible Wings at Low Speeds, Part IV -- Experimental Program and Comparison with Theory," VIDYA Report 172, Feb. 1965.

20. From unpublished study cited in Ref. 12.

21. Turner, M.J., Dill, E.H., Martin, H.C., and Melosh, R.J., "Large Deflections of Structures Subjected to Heating and External Loads," J. Aerospace Sci., 27:97-102, 127, 1960.

22. Argyris, J.H., Kesley, S., and Kamel, H., Matrix Methods of Structural Analysis," AGARDograph 72, Pergamon Press, Oxford, England, 1964.

23. Prezeminiecki, J.S., Theory of Matrix Structural Analysis, McGraw-Hill, New York, 1968.

24. Ormiston, Robert A., "Theoretical and Experimental Aerodynamics of an Elastic Sailwing," Ph.D. Thesis, Oct. 1969, Dept. of Aerospace and Mechanical Sciences, Princeton University, Princeton, N.J.

LIST OF SYMBOLS

Notation

[C]	Aerodynamic influence matrix (see appendix)
D	Displacement of panel nodes
E	Elasticity constant
EI	Bending rigidity
F	Force
K	Doublet strength
ℓ	Typical length
n	Unit vector normal to surface
P	Point on surface of sail
P	Pressure
p(x)	Loading on sail per unit length
q	Dynamic pressure
Re	Reynolds number
t	Sail thickness
[S]	Stiffness matrix
V	Fluid velocity
V_∞	Free-stream velocity
α	Angle of attack
β	Angle of side slip
γ	Vorticity
ϵ	Strain
ρ	Fluid density
σ	Stress
ϕ	Velocity perturbation potential
C_L	Lift coefficient

C_D	Drag coefficient
C_m	Pitching moment coefficient (based on keel length and referred to the $c_r/2$ point)
C_{m_α}	Slope of pitching moment curve with respect to α
C_{ℓ_β}	Effective dihedral (rolling moment coefficient due to yaw)
C_{n_β}	Yawing moment coefficient due to sideslip

Subscripts

e	elastic
f	full scale
g	geometric
i,j	indicies refer to individual panels
ℓ	lower surface
m	model
n	normal component
u	upper surfaces

TABLE 1

Details of Proposed Models

Configuration Number	Airframe*	Basic Design Features	Comments
1	A	High sweep, low aspect ratio, "standard"	For comparison with more recent designs and previous wind tunnel studies
2	B	High sweep, medium aspect ratio, 2° billow "intermediate"	Comparison with standard and high performance designs; effects of "billow"
3	C	High performance medium sweep (35°) zero tip chord	Washout not fixed by tips
4	C	Same as #3 with 45° sweep	Effect of sweep on stability
5	D	High performance low billow fixed minimum twist with "floating" ribs at tips	Effect of this common tip geometry on C_m
6	E	High performance low billow high twist dihedral	Features common to many contemporary hang gliders
7	E	Same as #6 with decreased twist	Effect of twist on performance and stability
8	E	Same as #6 without geometric dihedral	Dihedral effects on lateral stability and control response
9	E	Same as #6 with "keel pocket" and large reflex at root chord	Reflex effects on longitudinal stability and lateral control
10	F	Similar to #6 with low taper planform, low twist, reflex	Common to some of the highest performance gliders.

*Some configurations can be changed with minor model modifications, which results in the need for only 6 airframes for the 10 configurations listed.

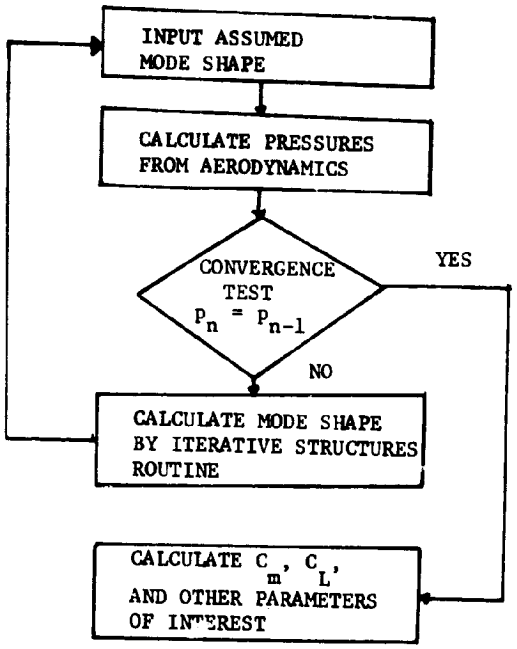

Figure 1.- Basic structure of load-prediction program.

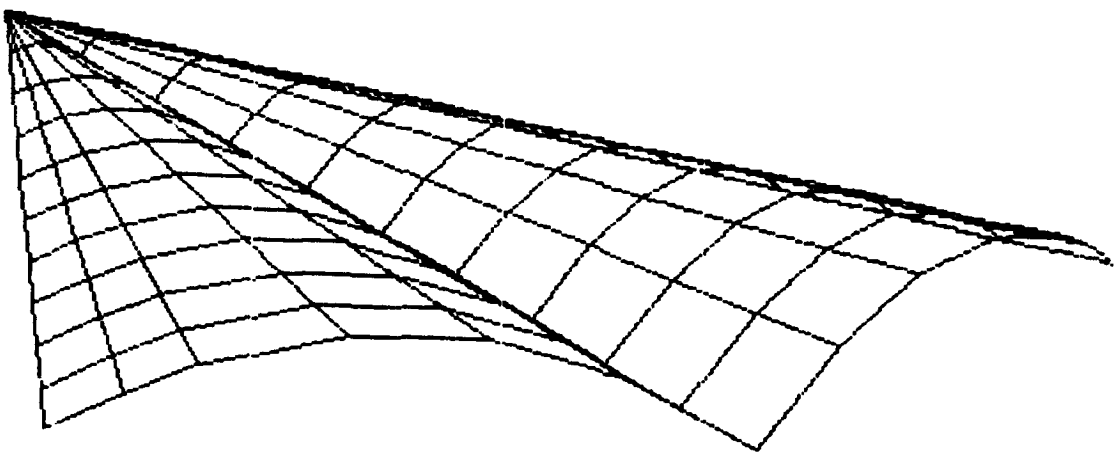

Figure 2.- Finite-element representation of hang glider sail.

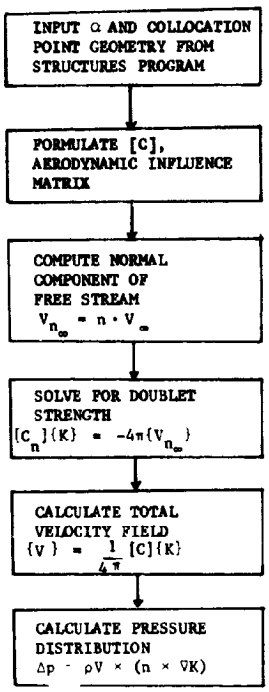

Figure 3.- Algorithm for aerodynamic analysis.

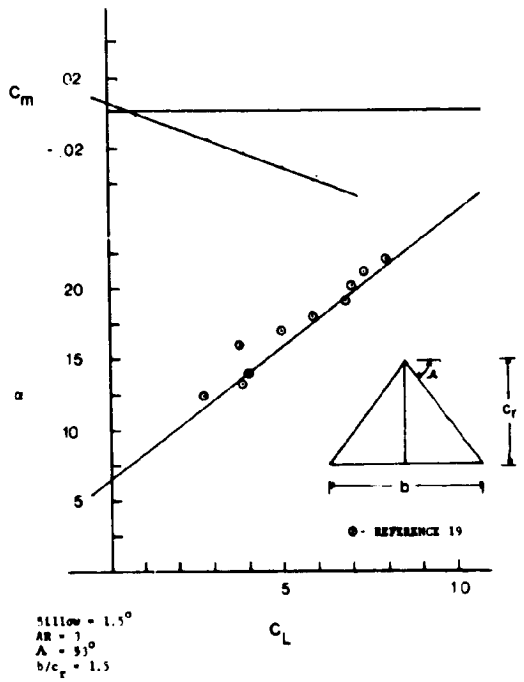

Figure 4.- Results of aerodynamic program.

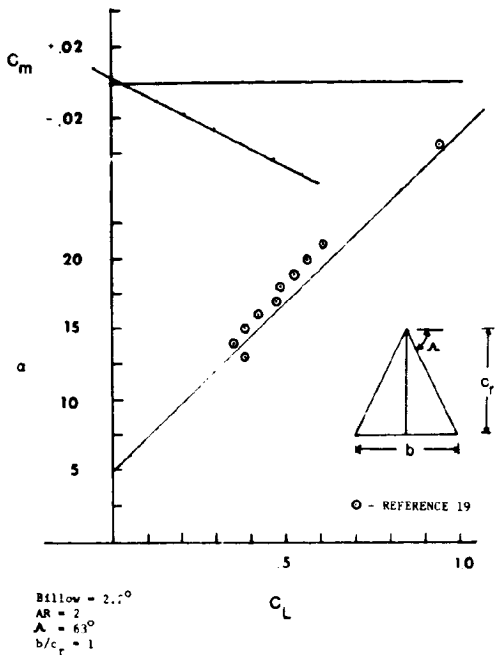

Figure 5.- Results of aerodynamic program.

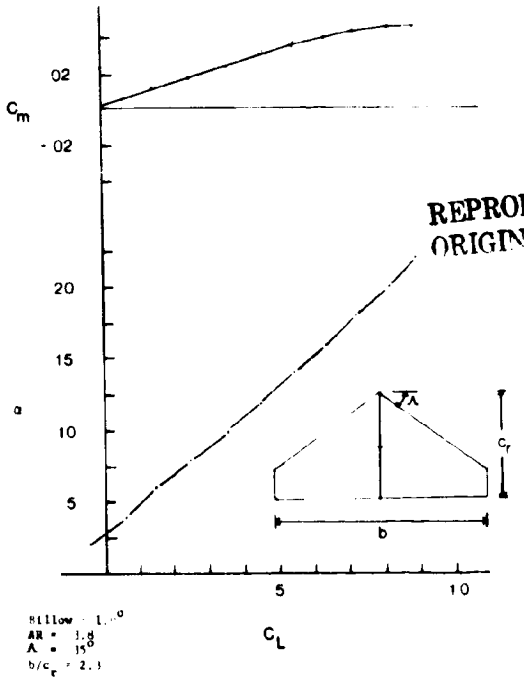

Figure 6.- Results of aerodynamic program.

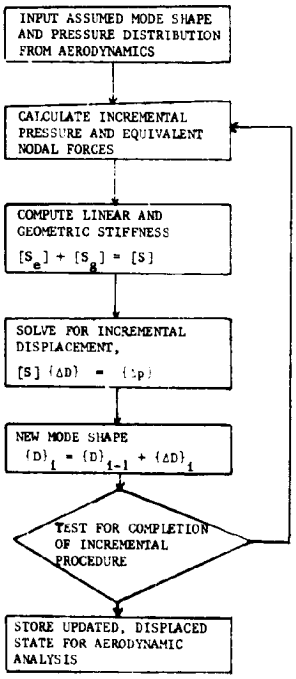

Figure 7.- Computational procedure — deflection analysis.